Optics and Laser Technology 103 (2018) 340–345

Contents lists available at ScienceDirect

Optics and Laser Technology

journal homepage: www.elsevier.com/locate/optlastec

Research Note

Patterning and reduction of graphene oxide using femtosecond-laser irradiation

SeungYeon Kang *,[1], Christopher C. Evans [2], Shobha Shukla [3], Orad Reshef [4], Eric Mazur

School of Engineering and Applied Sciences, Harvard University, Cambridge, MA 02138, USA

ARTICLE INFO

Article history:
Received 4 November 2017
Received in revised form 2 January 2018
Accepted 29 January 2018

ABSTRACT

Graphene has emerged as one of the most versatile materials ever discovered due to its extraordinary electronic, optical, thermal, and mechanical properties. However, device fabrication is a well-known challenge and requires novel fabrication methods to realize the complex integration of graphene-based devices. Here, we demonstrate direct laser writing of reduced graphene oxide using femtosecond-laser irradiation at $\lambda = 795$ nm. We perform a systematic study of the reduction process of graphene oxide to graphene by varying both the laser fluence and the pulse repetition rate. Our observations show that the reduction has both thermal and non-thermal features, and suggest that we can achieve better resolution and conductivity using kHz pulse trains than using MHz pulse trains or a continuous wave laser. Our reduced graphene oxide lines written at 10-kHz exhibit a 5 order-of-magnitude decrease in resistivity compared to a non-irradiated control sample. This study provides new insight into the reduction process of graphene oxide and opens doors to achieving a high degree of flexibility and control in the fabrication of graphene layers.

1. Introduction

Graphene is the thinnest and strongest material ever found with massless fermions and extraordinary thermal and electrical conductivity [1,2]. In order to make use of these properties in actual devices, fabrication techniques that produce patterned sub-micrometer features still need to be developed [3–6]. Current nanofabrication techniques for graphene are limited in resolution, dimension, or graphene quality [1–4,6,7]. Exfoliation and chemical reduction techniques are cost-effective and scalable but generate structural and chemical defects, leading to low-quality graphene sheets. These approaches cannot readily produce the shapes required for the fabrication of realistic devices and require additional steps for patterning [8–12]. Carbon nanotube unzipping methods produce high-quality graphene sheets but suffer from low throughput and lack of patterning abilities [13–16]. Chemical vapor deposition (CVD) and epitaxial growth methods permit large area, patterned production of graphene, but at a prohibitive cost. Additionally, the use of these methods is hindered by high temperature and vacuum requirements and a limited selection of suitable substrates [17–21]. Furthermore, the transfer process of CVD or epitaxially grown graphene layers to other substrates result in large surface roughness, folds, defects, and a decline in polarization-dependent absorption [21]. The development of reliable fabrication methods of high-quality graphene that are scalable and cost-effective for device fabrication is thus still an ongoing challenge.

In recent years, the photoreduction of graphene oxide to fabricate graphene has emerged as an appealing alternative because photoreduction does not rely on either high temperatures or toxic chemicals [3,22–23]. Photoreduction of graphene oxide by means of focused laser beams can produce patterned graphene structures [3,24–28]. The advantages of this technique are that it is reliable, scalable, cost-effective, and does not require the use of any predefined patterned masks for rapid-prototyping. Previous photoreduction work utilized UV, Hg, Xe lamps or continuous wave lasers in which the reduction mechanism resulted from linear absorption leading to thermal reduction [3,24–28]. Ultrafast optical pulses have been shown to induce material modification or chemical reactions through nonlinear absorption, but this approach remains largely unexplored [3,28,29].

In this communication, we use graphene oxide layers as templates to fabricate graphene patterns, and we systematically study

* Corresponding author.
E-mail address: sk32@princeton.edu (S. Kang).
[1] Current address: Mechanical and Aerospace Engineering, Princeton University, NJ 08540, USA.
[2] Current address: Laboratory of Atomic and Solid State Physics, Kavli Institute at Cornell for Nanoscale Science, Cornell University, Ithaca, NY 14853, USA.
[3] Current address: Metallurgical Engineering & Material Science, Indian Institute of Technology Bombay, Mumbai 400076, India.
[4] Current address: Advanced Research Complex 454, 25 Templeton Street, Ottawa ON K1N 6N5, Canada.

https://doi.org/10.1016/j.optlastec.2018.01.059
0030-3992/

the effect of ultrafast laser parameters on the reduction of graphene oxide to graphene to increase quality and achieve higher resolution patterning of graphene. Graphene oxide layers are easier to transfer to other substrates than graphene and permit the fabrication of thicker graphene layers [21]. We control the thermal vs. non-thermal reduction mechanism by varying the laser repetition rate, pulse duration, and laser fluence. We confirm the successful reduction of graphene oxide to graphene layers through optical images, X-ray photoelectron spectroscopy (XPS), and conductivity measurements. Our study suggests that we can obtain higher resolution and lower resistivity patterned graphite structures using a kHz-rate direct laser writing process.

2. Experimental procedures

2.1. Materials

We use commercial 170-nm-thick graphene oxide (GO) films (Graphene Laboratories Inc, NY, USA) deposited on 2-inch diameter glass substrates as the source material. For 4-probe conductivity measurements, we patterned gold contacts via optical lithography and electron-beam evaporation.

2.2. Laser fabrication

We use two different lasers to irradiate the samples: (1) a Ti:sapphire laser centered at 795 nm operating in either continuous-wave (CW) mode or in pulsed mode at an 11-MHz repetition rate, and a 300-fs pulse duration; (2) a Ti:sapphire laser centered at 794 nm operating at a 76-MHz, 10-kHz or 250-kHz repetition rate, with pulse durations of 125 fs, 180 fs or 400 fs. We adjust our laser spot sizes using different focal-length lenses to maintain similar spot sizes. For spot sizes of several tens of μm, we measure the spot size with a scanning-slit beam profiler after focusing the beam and placing the sample at the focus. To draw graphene lines and dashes, a high-precision 3-axis translation stage is used to select the region to be exposed and is translated at 10–100 μm/s to ensure full graphene-oxide reduction. We measure the spot size using the knife-edge method.

2.3. Characterization

We use optical microscopy and scanning electron microscopy (SEM) with an in-lens detector for post-fabrication characterization of structure dimensions. We analyze surface roughness using atomic force microscopy (AFM) and the elemental chemical composition of the surfaces using X-ray photoelectron spectroscopy (XPS). In the XPS analysis, the laser-reduced graphene oxide samples are compared with the untreated control graphene oxide films to identify the concentration of the remaining oxygen. To test the quality of the reduced graphene oxide structures, we perform conductivity measurements using a 4-probe station.

3. Results

We irradiate graphene oxide films with different laser parameters to determine the reduction threshold of graphene oxide using CW light and a train of femtosecond pulses with varying fluence and repetition rate. Fig. 1 is an example of the direct-laser-written reduced graphene oxide patterns after washing off the graphene oxide substrate. For the purposes of our study, we focus on patterned dots to compare the fabricated sample size for a given threshold power.

We expect the absorptive properties of the graphene oxide film to change as the film is reduced to graphene layers. By monitoring the normalized transmission of the laser through the sample during irradiation, we correlate transmission changes with material modification. We show several typical transmission versus time plots in Fig. 2. From observing the time-dependent transmission using different laser powers, we can identify two distinct regimes. In the first regime (Fig. 2, left), transmission decreases as a function of irradiation, indicating a modification in the material. The energy absorbed in this process likely contributes in the reduction of graphene oxide to graphene layers. At higher laser power, the transmission saturates faster with time, reaching a minimum value of 52%. At even higher laser power, we reach a second regime where the transmission rapidly increases with time, consistent with thinning of the material. We expect thinner material due to smaller inter-layer distance for graphene than graphene oxide. We use the term threshold power for the laser power required to obtain saturation behavior (minimum transmission) before thinning of the material within a 30-s laser exposure. For the case of Fig. 2, the threshold is 90 ± 10 mW. After laser modification, the laser-irradiated spots are observed using an optical microscope.

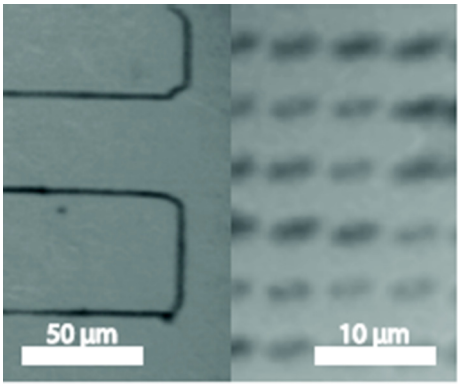

Fig. 1. SEM images of reduced graphene oxide lines (left) and dashes (right). A 76-MHz Ti:sapphire laser centered at 795 nm was used with an 0.65-NA objective lens. To draw lines and dashes, a high-precision 3-axis translation stage is used to select the region to be exposed and is translated at 100 μm/s.

3.1. CW laser irradiation

The laser spot size for CW laser irradiation is 35 μm in diameter. Fig. 2 shows the time-dependence of the transmission during irradiation at various laser powers. The left plot is representative of the first regime, where transmission of the reduced area decreases until saturation. The plot on the right shows the second regime, where transmission increases again. The threshold power of the film is 90 ± 10 mW. Fig. 3 shows optical images of the CW laser-irradiated spot. The diameter of the laser-modified area for a 100-mW irradiated sample is about 50 μm, significantly larger than the original laser spot size. This is consistent with material modification due to thermal effects. At 90 mW, we start seeing darker regions in the middle of the spots indicating formation of graphite layers, which we will discuss in more detail below.

3.2. 76-MHz laser irradiation

For the 76-MHz repetition-rate experiments, we used a pulse duration of 180 fs and a laser spot diameter of 35 μm. From the time dependence of the transmission for this irradiation (analogous to Fig. 2), we identify a threshold power of about 60 mW. Optical images show that the diameter of the laser modified area is 40 μm, comparable to the original laser spot size. Dark regions in the middle of the irradiate area appear at laser powers of 60 mW.

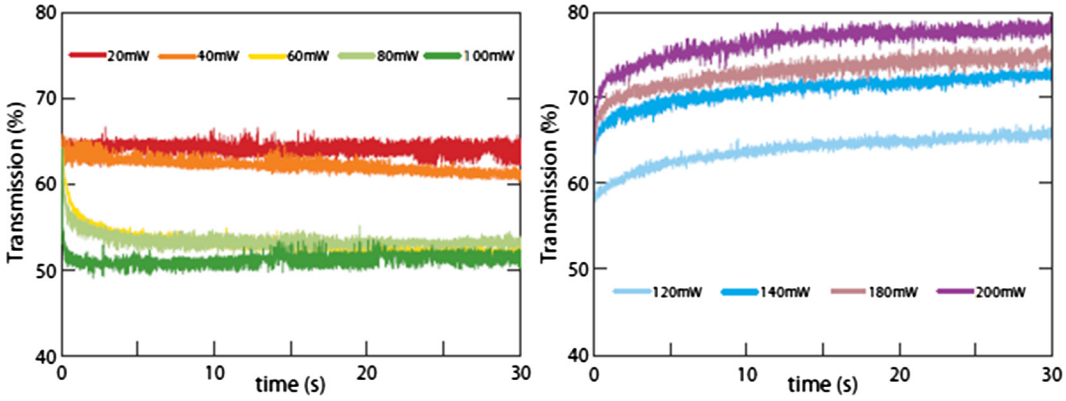

Fig. 2. Time-dependence of the transmission during irradiation with a CW laser at various average powers. Left: regime prior to transmission saturation, indicating a material modification. Right: material ablation.

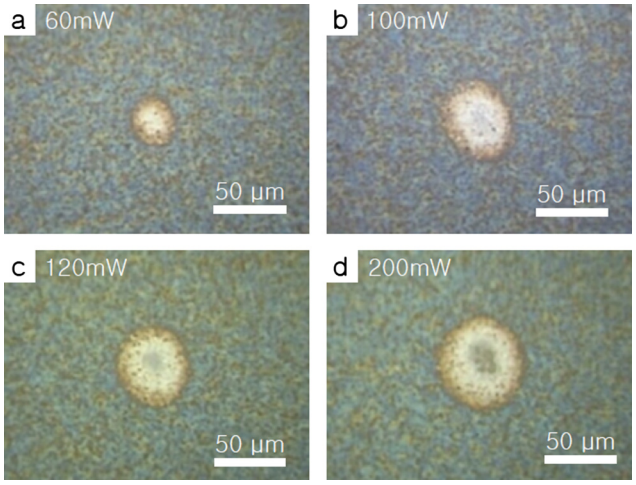

Fig. 3. Optical images of CW laser irradiated spots at various laser powers. (a) optical image of a sample area from the first regime prior to transmission saturation, indicating material modification. (b, c, d) optical images of the sample areas from the second regime, indicating graphene formation then the ablation of the material.

3.3. 250-kHz laser irradiation

At 250 kHz, we use pulse durations of 400 fs and 125 fs and a laser spot size of 35 μm. The threshold power of the film is around 30 mW for 400-fs pulses and 15 mW for 125-fs pulses; the average diameter of the laser-modified area is about 40 μm for 400-fs pulses and 35 μm for 125-fs pulses. Dark areas appear at laser powers corresponding to threshold powers and can be seen in the 60-mW and 10-mW optical images, respectively.

3.4. 10-kHz laser irradiation

At 10 kHz, we use a pulse duration of 180 fs and a laser spot size of 150 μm. The threshold power is around 10 mW and the diameter of the laser-modified area is about 40 μm, which is close to a quarter of the original laser spot size. Dark areas appear at 10 mW. All of these data are summarized in Table 1.

3.5. Surface analysis

We use AFM to further probe the structural properties of the laser-irradiated spots. Fig. 4 is an AFM image and a surface height plot of a cross-section across the middle of the laser irradiated area for a 76-MHz laser irradiated sample at 90 mW. Considering that graphene oxide has similar structure to graphite with much wider spacing (0.6–1.2 nm) between layers due to its hygroscopic nature [4,30], we expect a much thinner layer of 2D graphite in the laser irradiated areas from the reduction of the functional groups between the graphene layers. Indeed, the laser-irradiated area is thinner than the non-irradiated area, as one would expect from the reduction of graphene oxide layers.

To determine whether laser irradiation leads to a reduction of the graphene oxide, we performed XPS measurements. Fig. 5 show XPS data obtained from a sample irradiated with a 140-mW CW laser over a 50-μm sized area. The decrease in the C—O bonding peak in the reduced graphene oxide sample in the left plot of Fig. 5 is indicative of a reduction of the graphene oxide layer. The remaining C—O and C=O bonding peaks can be attributed to the non-irradiated area, as the theoretical spatial resolution of the XPS is only 50 μm. In addition to the decrease in C—O bonds, we observe a peak shift in the C—C bonding signal to a lower energy. This shift is in qualitative agreement with an increase of sp2 bonding (a unique characteristic of a defect free and pure graphene) which has a slightly lower binding energy than the sp3 bonding in graphene oxide. Unfortunately the XPS resolution is too low to fit individual sp2 and sp3 in the reduced graphene oxide data.

We also measure the conductivity of the patterned graphene structures. After evaporating rectangular gold contacts on the structures, we carry out a 4-point probe measurement. Fig. 6a shows an SEM image of a direct laser-written graphite line with the 4-point probe contacts. Scratches on the gold contacts are

Table 1
Summary of results. Spot size is the diameter of the laser beam on the sample and sample size is the diameter of the laser-modified area. Threshold peak intensity is the calculated peak intensity of the threshold power values acquired from the time-dependence of the transmission of the irradiated samples.

Laser type	Pulse duration (fs)	Energy threshold (mW)	Spot size (μm)	Sample size (μm)	Threshold peak intensity (W/m^2)
CW	–	90	35	50	9.36×10^7
76 MHz	180	60	35	45	4.33×10^{12}
250 kHz 400-fs pulse	400	30	35	40	3.12×10^{14}
250 kHz 125-fs pulse	125	15	35	35	4.99×10^{14}
10 kHz	180	10	150	40	3.14×10^{14}

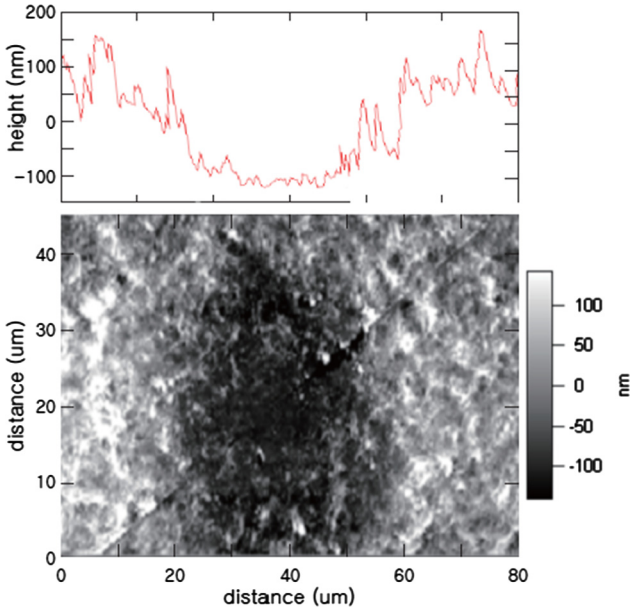

Fig. 4. AFM image of a 76-MHz laser irradiated area (bottom). The top plot is a cross section across the middle section of the AFM image. (The diagonal line in the image is an artifact of the imaging software.)

due to the probes during the conductivity measurement. The graphene line in the image was written at a speed of 10 μm/s, a repetition rate of 10 kHz, and pulse duration of 200 fs.

Fig. 6b shows the resistance measured for the direct laser written lines using the setup in Fig. 6(a). Control is the resistance of an unaltered GO sample. For the CW experiment, we produced 2–4-μm-wide lines with a spot size of 1 μm and writing speed of 10–100 μm/s at 34 mW. We varied the writing speed to ensure full reduction. The 11-MHz experiment also had a spot size of 1 μm with a writing speed of 100 μm/s at 32 mW and it resulted in 1–2-μm wide lines. For the 10-kHz experiment, we produced 1–2-μm wide lines with a spot size of 5 μm at writing speeds of 10–100 μm/s and 40 mW. We tested writing speeds of 10–100 μm/s to confirm we achieve the threshold power when writing the lines. As the data show, lines written at 10-kHz exhibit a 5 order-of-magnitude decrease in resistivity compared to a non-irradiated control sample.

4. Discussion

Table 1 summarizes our results. The threshold peak intensity increases as the repetition rate is decreased, with irradiation at a low repetition rate (250 kHz and 10 kHz) yielding two orders of magnitude larger peak intensities than irradiation at a high repetition rate (76-MHz). The large differences in the peak intensities suggest that CW and 76-MHz laser irradiation result from a ther-

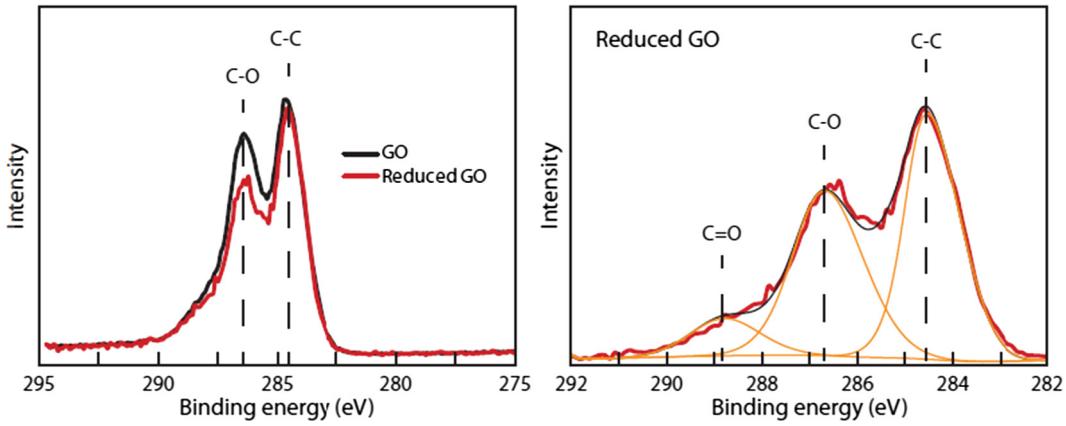

Fig. 5. XPS of a 140-mW CW laser irradiated sample. The left plot compares non-irradiated control sample with the irradiated sample and the right plot is a magnified view of the result.

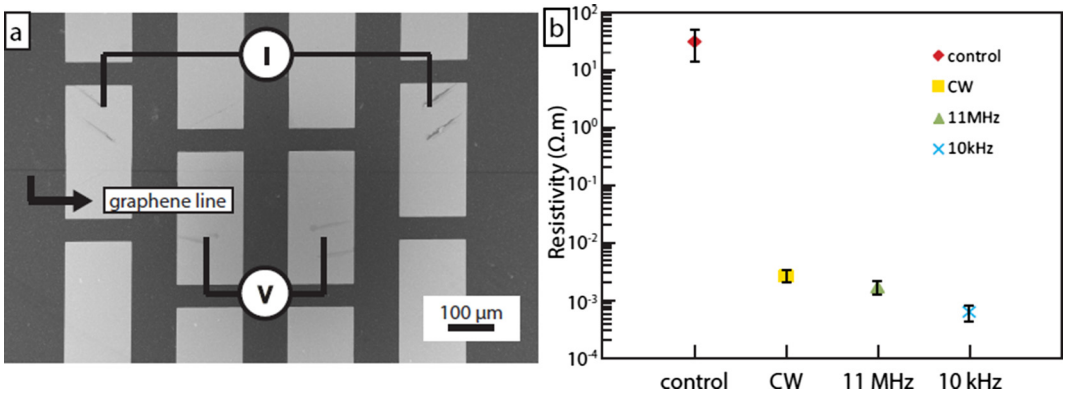

Fig. 6. (a) SEM image showing graphene line with a 4-point probe schematic. Each gold contact is 150 μm × 300 μm. Writing speed of 10 μm/s, repetition rate of 10 kHz and pulse duration of 200 fs were used to write this specific line. (b) Resistance of various direct laser written lines. (y axis is on a log scale and x axis lists the different types of lasers used.)

mal mechanism mediated by linear-absorption, while the 250-kHz irradiation involves both linear and nonlinear (multiphoton) absorption in the reduction of graphene oxide. We also note that the fabricated sample size is largest for CW irradiation and increases with the use of longer pulses. This trend is another indication that thermal accumulation during CW and low repetition-rate irradiation with long pulse durations causes the larger modified areas that we observe. At 10 kHz, the sample size is approximately a quarter of the laser spot size. Given that the repetition-rate is more than 10 times lower than at 250 kHz, the large difference in sample size suggests that at 10 kHz the graphene reduction is due to nonlinear optical photoreduction only rather than a combination of both linear and nonlinear photoreduction. At 10 kHz, we obtain the highest beam-spot to sample-size ratio, larger than any previously reported results [22–25]. Furthermore, the measured conductivity also indicates that the patterned graphene at 10 kHz has a resistivity of just $(6.3 \pm 1.8) \times 10^{-4}\ \Omega$.m, which is 5 orders of magnitude lower than the unreduced graphene oxide. This resistivity value refers to $(1.5 \pm 0.5) \times 10^{3}$ S m^{-1} in conductivity. While we find our value is one order of magnitude higher in resistivity and comparable or three orders of magnitude lower in conductivity than previous reports ($3.9 \times 10^{-5}\ \Omega$.m Ref. [25], 1.73 8×10^{3} Sm^{-1} Ref. [31], 1.1×10^{6} Sm^{-1} Ref. [32]), we attribute this difference to the quality of our original graphene oxide substrate. This suggests that the purely nonlinear photoreduction at 10 kHz results in better resolution and minimal thermal degradation of the material. Finally, time-dependence of the transmission shows that it takes longer to reach saturation at the lower repetition rates.

5. Conclusion

In summary, we investigated the reduction of graphene oxide using femtosecond laser irradiation. We demonstrate direct laser writing of reduced graphene oxide structures and explore the reduction process over a range of laser fluences and repetition rates (from continuous wave to 76 MHz). By comparing the threshold powers required for graphene oxide modification and the size of the resulting structures, we can decouple thermal and non-thermal reduction. The direct laser-writing technique yields 1–2-μm-wide graphene lines with a 5 order of magnitude decrease in resistivity. This leads us to believe that graphene formation using nonlinear laser irradiation may provide more control over resolution and quality of the reduced graphene oxide structures when compared with conventional fabrication techniques, opening the door to achieving a high degree of flexibility and control in the fabrication of graphene layers.

Funding and Acknowledgement

Several people contributed to the work described in this paper. C.E and S.S conceived of the basic idea for this work. S.K. developed the idea, designed and carried out the experiments, and analyzed the results. O.R. fabricated the gold contact pads. E.M. supervised the research and the development of the manuscript. S.K. wrote the first draft of the manuscript; all authors subsequently took part in the revision process and approved the final copy of the manuscript. The research described in this paper was supported by the Air Force Office of Scientific Research under Grants FA9550-09-1-0546 and FA9550-10-1-0402. The authors acknowledge the use of facilities in the Center for Nanoscale Systems, which is supported by the National Science Foundations National Nanotechnology Infrastructure Network.

References

[1] A.K. Geim, K.S. Novoselov, The rise of graphene, Nature Mater. 6 (3) (2007) 183–191.
[2] A.K. Geim, Graphene: status and prospects, Science 324 (2009) 1530–1534.
[3] Yong-Lai Zhang, Li Guo, Hong Xia, Qi-Dai Chen, Jing Feng, Hong-Bo Sun, Photoreduction of graphene oxides: methods, properties, and applications, Adv. Optical Mater. 2 (1) (2014) 10–28.
[4] Daniel R Dreyer, Sungjin Park, Christopher W. Bielawski, Rodney S. Ruoff, The chemistry of graphene oxide, Chem. Soc. Rev. 39(1) (2010) 228–240.
[5] Sungjin Park, Jinho An, Inhwa Jung, Richard D Piner, Sung Jin An, Xuesong Li, Aruna Velamakanni, Rodney S. Ruoff, Colloidal suspensions of highly reduced graphene oxide in a wide variety of organic solvents, Nano Lett. 9(4) (2009) 1593–1597.
[6] Boya Dai, Fu. Lei, Lei Liao, Nan Liu, Kai Yan, Yongsheng Chen, Zhongfan Liu, High-quality single-layer graphene via reparative reduction of graphene oxide, Nano Res. 4 (5) (2011) 434–439.
[7] Sungjin Park, Rodney S. Ruoff, Chemical methods for the production of graphenes, Nature Nanotechnol. 4 (4) (2009) 217–224.
[8] Du. Wencheng, Xiaoqing Jiang, Lihua Zhu, From graphite to graphene: direct liquid-phase exfoliation of graphite to produce single- and few-layered pristine graphene, J. Mater. Chem. A 1 (36) (2013) 10592.
[9] Mustafa Lotya, Yenny Hernandez, Paul J King, Ronan J. Smith, Valeria Nicolosi, Lisa S. Karlsson, Fiona M. Blighe, Sukanta De, Zhiming Wang, I T McGovern, Georg S. Duesberg, Jonathan N. Coleman, Liquid phase production of graphene by exfoliation of graphite in surfactant/water solutions, J. Am. Chem. Soc. 131 (10) (2009) 3611–3620.
[10] Jonathan N. Coleman, Liquid-phase exfoliation of nanotubes and graphene, Adv. Funct. Mater. 19 (23) (2009) 3680–3695.
[11] Jonathan N. Coleman, Liquid exfoliation of defect-free graphene, Accounts Chem. Res. 46(1) (2013) 14–22.
[12] Yenny Hernandez, Valeria Nicolosi, Mustafa Lotya, Fiona M. Blighe, Zhenyu Sun, Sukanta De, I T McGovern, Brendan Holland, Michele Byrne, Yurii K. Gun'Ko, John J. Boland, Peter Niraj, Georg Duesberg, Satheesh Krishnamurthy, Robbie Goodhue, John Hutchison, Vittorio Scardaci, Andrea C. Ferrari, Jonathan N. Coleman, High-yield production of graphene by liquid-phase exfoliation of graphite, Nature Nanotechnol. 3(9) (2008) 563–568.
[13] Dmitry V Kosynkin, Amanda L Higginbotham, Alexander Sinitskii, Jay R. Lomeda, Ayrat Dimiev, B. Katherine Price, James M. Tour, Longitudinal unzipping of carbon nanotubes to form graphene nanoribbons, Nature 458 (7240) (2009) 872–876.
[14] Alexander Sinitskii, Ayrat Dimiev, Dmitry V. Kosynkin, James M. Tour, Graphene nanoribbon devices produced by oxidative unzipping of carbon nanotubes, ACS Nano 4(9) (2010) 5405–5413.
[15] Dhanraj B. Shinde, Joyashish Debgupta, Ajay Kushwaha, Mohammed Aslam, Vijayamohanan K. Pillai, Electrochemical unzipping of multi-walled carbon nanotubes for facile synthesis of high-quality graphene nanoribbons, J. Am. Chem. Soc. 133(12) (2011) 4168–4171.
[16] S. Mohammadi, Z. Kolahdouz, S. Darbari, S. Mohajerzadeh, N. Masoumi, Graphene formation by unzipping carbon nanotubes using a sequential plasma assisted processing, Carbon 52 (2013) 451–463.
[17] Keun Soo Kim, Yue Zhao, Houk Jang, Sang Yoon Lee, Jong Min Kim, Kwang S. Kim, Jong-Hyun Ahn, Philip Kim, Jae-Young Choi, Byung Hee Hong, Large-scale pattern growth of graphene films for stretchable transparent electrodes, Nature 457(7230) (2009) 706–710.
[18] Ariel Ismach, Clara Druzgalski, Samuel Penwell, Adam Schwartzberg, Maxwell Zheng, Ali Javey, Jeffrey Bokor, Yuegang Zhang, Direct chemical vapor deposition of graphene on dielectric surfaces, Nano Lett. 10 (5) (2010) 1542–1548.
[19] Alfonso Reina, Xiaoting Jia, John Ho, Daniel Nezich, Hyungbin Son, Vladimir Bulovic, Mildred S. Dresselhaus, Jing Kong, Large area, few-layer graphene films on arbitrary substrates by chemical vapor deposition, Nano Lett. 9(1) (2009) 30–35.
[20] Iskandar N. Kholmanov, Carl W Magnuson, Ali E. Aliev, Huifeng Li, Bin Zhang, Ji Won Suk, Li Li Zhang, Eric Peng, S. Hossein Mousavi, Alexander B. Khanikaev, Richard Piner, Gennady Shvets, Rodney S. Ruoff, Improved electrical conductivity of graphene films integrated with metal nanowires, Nano Lett. 12(11) (2012) 5679–5683.
[21] Fei Xing, Gui-Xian Meng, Qian Zhang, Lei-Ting Pan, Peng Wang, Zhi-Bo Liu, Wen-Shuai Jiang, Yongsheng Chen, Jian-Guo Tian, Ultrasensitive flow sensing of a single cell using graphene-based optical sensors, Nano Lett. 14 (6) (2014) 3563–3569.
[22] Kymakis, Emmanuel, et al. Flexible organic photovoltaic cells with in situ nonthermal photoreduction of spin-coated graphene oxide electrodes, Adv. Funct. Mater. 23(21) (2013) 2742–2749.
[23] Li, Xiangping, et al. Athermally photoreduced graphene oxides for three-dimensional holographic images, Nature Commun. 6 (2015).
[24] Hong Zhang, Yoshiyuki Miyamoto, Graphene production by laser shot on graphene oxide: an ab initio prediction, Phys. Rev. B 85 (3) (2012) 033402.
[25] Denis A. Sokolov, Kristin R. Shepperd, Thomas M. Orlando, Formation of graphene features from direct laser-induced reduction of graphite oxide, J. Phys. Chem. Lett. 1 (18) (2010) 2633–2636.
[26] Wei Gao, Neelam Singh, LiSong, Zheng Liu, Arava Leela Mohana Reddy, Lijie Ci, Robert Vajtai, Qing Zhang, Bingqing Wei, Pulickel M. Ajayan, Direct laser

writing of micro-supercapacitors on hydrated graphite oxide films, Nature Nanotechnol. 6(8) (2011) 496–500.
[27] By Yong Zhou, Qiaoliang Bao, Binni Varghese, Lena Ai Ling Tang, Chow Khim Tan, Chorng-Haur Sow, Kian Ping Loh, Microstructuring of graphene oxide nanosheets using direct laser writing, Adv. Mater. 22(1) (2010) 67–71.
[28] Yonglai Zhang, Li Guo, Shu Wei, Yinyan He, Hong Xia, Qidai Chen, Hong-Bo Sun, Feng-Shou Xiao, Direct imprinting of microcircuits on graphene oxides film by femtosecond laser reduction, Nano Today 5 (1) (2010) 15–20.
[29] Bohdan Senyuk, Natnael Behabtu, Angel Martinez, Taewoo Lee, Dmitri E. Tsentalovich, Gabriel Ceriotti, James M. Tour, Matteo Pasquali, Ivan I. Smalyukh, Three-dimensional patterning of solid microstructures through laser reduction of colloidal graphene oxide in liquid-crystalline dispersions, Nature Commun. 6 (7157) (2015).
[30] Alexandra Buchsteiner, Anton Lerf, Jörger Pieper, Water dynamics in graphite oxide investigated with neutron scattering, J. Phys. Chem. B. 110 (45) (2006) 22328–22338.
[31] Maher F. El-Kady, Veronica Strong, Sergey Dubin, Richard B. Kaner, Laser Scribing of High-performance and flexible graphene-based electrochemical capacitors, Science 335 (6074) (2012) 1326–1330.
[32] R.-Z.Li,Rui Peng, K.D. Kihm, S. Bai, D. Bridges, U. Tumuluri, Z. Wu, T. Zhang, G. Compagnini, Z. Feng, A. Hu, High-rate in plane micro-supercapacitors scribed onto photo paper using in situ femtolaser-reduced graphene oxide/Au nanoparticle microelectrodes, Energy & Environ. Sci. 9 (2016) 1458–1467.